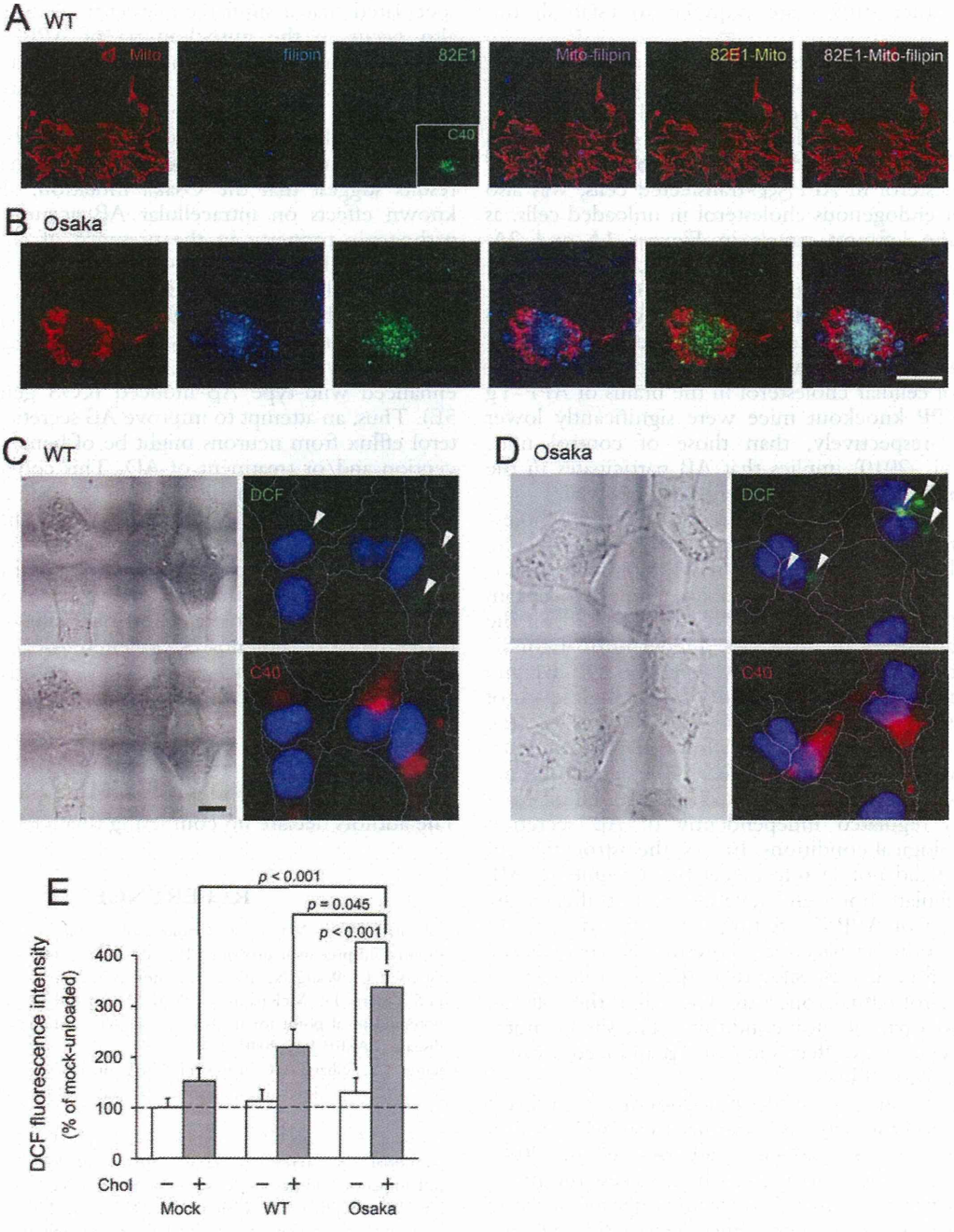


Fig. 5. Mitochondrial accumulation of Aβ and cholesterol and ROS generation in $APP_{OSK}$-expressing cells. COS-7 cells were transfected with an $APP_{WT}$ (A,C) or $APP_{OSK}$ (B,D) construct and loaded with cholesterol. Mitochondrial localization of cholesterol and Aβ was examined with filipin (blue), 82E1 antibody (green), and mitotracker (red). APP expression was confirmed with C40 antibody (A **inset**, green). **A:** In $APP_{WT}$-expressing cells, only a few filipin-positive punctae were observed and almost no localization of cholesterol at the mitochondria. **B:** In $APP_{OSK}$-expressing cells, a portion of cholesterol and Aβ accumulated in the mitochondria, and these materials were partially colocalized. **C,D:** For the visualization of intracellular ROS, cells were stained with carboxy $H_2$DCFDA, followed by counterstaining with Hoechst 33342. Phase-contrast images and DCF fluorescence (green, arrowheads) were taken before cell fixation (upper rows in C,D). The cells were then fixed and stained with C40 antibody to confirm APP expression (red, lower rows). **E:** Intracellular ROS was quantified by measuring DCF fluorescence with a multiplate reader. Cholesterol loading considerably increased ROS levels in all cells. The increased ROS generation induced by cholesterol loading was much greater in $APP_{OSK}$-transfected cells than in mock- and $APP_{WT}$-transfected cells. Results are presented as mean ± SEM (n = 8). Scale bar = 10 micrometer in B (applies to A, B) and C (applies to C, D).

the cell. Further studies are required to establish this conclusion.

The effect of the Osaka mutation on intracellular cholesterol transport and efflux was clearly demonstrated here in cultured cells after exogenous cholesterol loading. The same tendency, i.e., lower levels of cellular cholesterol in $APP_{WT}$-transfected cells and unchanged levels of cellular cholesterol in $APP_{OSK}$-transfected cells, was also observed for endogenous cholesterol in unloaded cells, as shown in the leftmost panels in Figures 1A and 2A, although the changes were relatively mild. It may be that Aβ functions in particular to correct an abnormal increase of cellular cholesterol levels, so its effect was not so evident when cellular cholesterol levels were in the normal range. However, our previous observation that steady-state levels of cellular cholesterol in the brains of APP-Tg mice and APP knockout mice were significantly lower and higher, respectively, than those of control mice (Umeda et al., 2010) implies that Aβ participates in the regulation of endogenous cholesterol levels as well.

In the brain, astrocytes play a critical role in cholesterol turnover (Pfrieger and Ungerer, 2011). They secrete HDL-type lipoproteins to deliver newly synthesized cholesterols to neurons and collect extra cholesterols from neurons for their redistribution. Neurons depend on the supply of cholesterol by astrocytes. Under normal conditions, astrocytes express very low levels of BACE1 and thus produce very little Aβ in spite of their high levels of APP expression (Zhao et al., 1996; Rossner et al., 2001); astrocytes come to express BACE1 when they are activated (Hartlage-Rübsamen et al., 2003; Hong et al., 2003). These findings suggest that cholesterol efflux from astrocytes is regulated independently of Aβ secretion under physiological conditions. In fact, the astrocytic cells that we used did not secrete detectable amounts of Aβ, and their cellular choresterol levels were not affected by the expression of APP. In resting-state astrocytes, apoE, ABCA1, and other factors, if any, presumably mediate the cholesterol efflux. It is possible that Aβ has a role to promote cholesterol efflux from astrocytes when the cells are activated under pathological conditions. The Osaka mutation in astrocytes may affect such an Aβ-induced promotion of cholesterol efflux.

It has been shown that the mitochondria are a direct site for Aβ accumulation in neurons from AD patients and transgenic mouse models (Caspersen et al., 2005; Manczak et al., 2006). Aβ is thought to access the mitochondrial matrix via intracellular trafficking and mediate mitochondrial toxicity, including metabolic enzyme defects, respiratory chain dysfunction, and ROS generation (Caspersen et al., 2005; Manczak et al., 2006). We have demonstrated that Aβ that accumulated in the mitochondria causes mitochondrial dysfunction and subsequent cell death in $APP_{OSK}$-transfected cells and the brains of $APP_{OSK}$-Tg mice (Umeda et al., 2011). Another study has shown that mitochondrial cholesterol increases the susceptibility of neurons to $A\beta_{42}$-induced oxidative stress, probably by a cholesterol-mediated depletion of mitochondrial glutathione (Fernandez et al., 2009). We speculated that a similar cholesterol accumulation might also occur in the mitochondria of $APP_{OSK}$-expressing cells upon cholesterol loading, which would enhance Aβ-induced ROS generation. Supporting this theory, we detected an increase in the accumulation of cholesterol and Aβ in the mitochondria of $APP_{OSK}$-expressing cells and an accompanying increase in ROS generation. These results suggest that the Osaka mutation, along with its known effects on intracellular Aβ accumulation, has a pathogenic property in the presence of cholesterol that sensitizes cells to oxidative stress. We have also observed that the Osaka mutation-induced pathology can be accelerated by hypercholesterolemia in $APP_{OSK}$-Tg mice (Umeda et al., 2012). Evidence here suggests that this might apply to $APP_{WT}$ as well, because cholesterol enhanced wild-type Aβ-induced ROS generation (Fig. 5E). Thus, an attempt to improve Aβ secretion and cholesterol efflux from neurons might be of benefit for the prevention and/or treatment of AD. This could be achieved by stimulation of synaptic activity (Tampellini et al., 2009) by means of learning, exercise, and so on. Antioxidants and cholesterol-lowering medicine would also be effective for attenuating intracellular Aβ toxicity. In summary, the present findings suggest that Aβ trafficking is important for intracellular cholesterol transport and efflux and that the Osaka mutation potentiates cholesterol-dependent exacerbation of intracellular Aβ toxicity by disturbing Aβ-mediated cholesterol efflux from the cell.

## ACKNOWLEDGMENTS

The authors declare no conflicting financial interests.

## REFERENCES

Bodovitz S, Klein WL. 1996. Cholesterol modulates α-secretase cleavage of amyloid precursor protein. J Biol Chem 271:4436–4440.

Caspersen C, Wang N, Yao J, Sosunov A, Chen X, Lustbader JW, Xu HW, Stern D, McKhann G, Yan SD. 2005. Mitochondrial Aβ: a potential focal point for neuronal metabolic dysfunction in Alzheimer's disease. FASEB J 19:2040–2041.

Chang TY, Chang CC, Ohgami N, Yamauchi Y. 2006. Cholesterol sensing, trafficking, and esterification. Annu Rev Cell Dev Biol 22: 129–157.

Fernandez A, Llacuna L, Fernandez-Checa JC, Colell A. 2009. Mitochondrial cholesterol loading exacerbates amyloid β peptide-induced inflammation and neurotoxicity. J Neurosci 29:6394–6405.

Frears ER, Stephens DJ, Walters CE, Davies H, Austen BM. 1999. The role of cholesterol in the biosynthesis of β-amyloid. Neuroreport 10: 1699–1705.

Hartlage-Rübsamen M, Zeitschel U, Apelt J, Gärtner U, Franke H, Stahl T, Günther A, Schliebs R, Penkowa M, Bigl V, Rossner S. 2003. Astrocytic expression of the Alzheimer's disease β-secretase (BACE1) is stimulus-dependent. Glia 41:169–179.

Hong HS, Hwang EM, Sim HJ, Cho HJ, Boo JH, Oh SS, Kim SU, Mook-Jung I. 2003. Interferon γ stimulates β-secretase expression and sAPPβ production in astrocytes. Biochem Biophys Res Commun 307: 922–927.

Manczak M, Anekonda TS, Henson E, Park BS, Quinn J, Reddy PH. 2006. Mitochondria are a direct site of Aβ accumulation in Alzheimer's

disease neurons: implications for free radical generation and oxidative damage in disease progression. Hum Mol Genet 15:1437–1449.

Nishitsuji K, Tomiyama T, Ishibashi K, Ito K, Teraoka R, Lambert MP, Klein WL, Mori H. 2009. The E693Δ mutation in amyloid precursor protein increases intracellular accumulation of amyloid β oligomers and causes endoplasmic reticulum stress-induced apoptosis in cultured cells. Am J Pathol 174:957–969.

Pfrieger FW, Ungerer N. 2011. Cholesterol metabolism in neurons and astrocytes. Prog Lipid Res 50:357–371.

Prinz WA. 2007. Non-vesicular sterol transport in cells. Prog Lipid Res 46:297–314.

Rossner S, Apelt J, Schliebs R, Perez-Polo JR, Bigl V. 2001. Neuronal and glial β-secretase (BACE) protein expression in transgenic Tg2576 mice with amyloid plaque pathology. J Neurosci Res 64: 437–446.

Solomon A, Kivipelto M. 2009. Cholesterol-modifying strategies for Alzheimer's disease. Expert Rev Neurother 9:695–709.

Stefani M, Liguri G. 2009. Cholesterol in Alzheimer's disease: unresolved questions. Curr Alzheimer Res 6:15–29.

Subramanian K, Balch WE. 2008. NPC1/NPC2 function as a tag team duo to mobilize cholesterol. Proc Natl Acad Sci U S A 105:15223–15224.

Suga K, Tomiyama T, Mori H, Akagawa K. 2004. Syntaxin 5 interacts with presenilin holoproteins, but not with their N- or C-terminal fragments, and affects β-amyloid peptide production. Biochem J 381:619–628.

Tampellini D, Rahman N, Gallo EF, Huang Z, Dumont M, Capetillo-Zarate E, Ma T, Zheng R, Lu B, Nanus DM, Lin MT, Gouras GK. 2009. Synaptic activity reduces intraneuronal Aβ, promotes APP transport to synapses, and protects against Aβ-related synaptic alterations. J Neurosci 29:9704–9713.

Tomiyama T, Nagata T, Shimada H, Teraoka R, Fukushima A, Kanemitsu H, Takuma H, Kuwano R, Imagawa M, Ataka S, Wada Y, Yoshioka E, Nishizaki T, Watanabe Y, Mori H. 2008. A new amyloid β variant favoring oligomerization in Alzheimer's-type dementia. Ann Neurol 63:377–387.

Tomiyama T, Matsuyama S, Iso H, Umeda T, Takuma H, Ohnishi K, Ishibashi K, Teraoka R, Sakama N, Yamashita T, Nishitsuji K, Ito K, Shimada H, Lambert MP, Klein WL, Mori H. 2010. A mouse model of amyloid β oligomers: their contribution to synaptic alteration, abnormal tau phosphorylation, glial activation, and neuronal loss in vivo. J Neurosci 30:4845–4856.

Umeda T, Mori H, Zheng H, Tomiyama T. 2010. Regulation of cholesterol efflux by amyloid β secretion. J Neurosci Res 88:1985–1994.

Umeda T, Tomiyama T, Sakama N, Tanaka S, Lambert MP, Klein WL, Mori H. 2011. Intraneuronal amyloid β oligomers cause cell death via endoplasmic reticulum stress, endosomal/lysosomal leakage, and mitochondrial dysfunction in vivo. J Neurosci Res 89:1031–1042.

Umeda T, Tomiyama T, Kitajima E, Idomoto T, Nomura S, Lambert MP, Klein WL, Mori H. 2012. Hypercholesterolemia accelerates intraneuronal accumulation of Aβ oligomers resulting in memory impairment in Alzheimer's disease model mice. Life Sci 91:1169–1176.

Xiong H, Callaghan D, Jones A, Walker DG, Lue LF, Beach TG, Sue LI, Woulfe J, Xu H, Stanimirovic DB, Zhang W. 2008. Cholesterol retention in Alzheimer's brain is responsible for high β- and γ-secretase activities and Aβ production. Neurobiol Dis 29:422–437.

Yokoyama S. 2006. Assembly of high-density lipoprotein. Arterioscler Thromb Vasc Biol 26:20–27.

Zhao J, Paganini L, Mucke L, Gordon M, Refolo L, Carman M, Sinha S, Oltersdorf T, Lieberburg I, McConlogue L. 1996. β-Secretase processing of the β-amyloid precursor protein in transgenic mice is efficient in neurons but inefficient in astrocytes. J Biol Chem 271:31407–31411.

Neuroscience Letters 534 (2013) 85–89

Contents lists available at SciVerse ScienceDirect

Neuroscience Letters

journal homepage: www.elsevier.com/locate/neulet

# Proteomic analysis of the hippocampus in Alzheimer's disease model mice by using two-dimensional fluorescence difference in gel electrophoresis

Masaoki Takano[a], Takuya Yamashita[b,c], Kazuya Nagano[c], Mieko Otani[a], Kouji Maekura[a], Haruhiko Kamada[c], Shin-ichi Tsunoda[c], Yasuo Tsutsumi[b,c], Takami Tomiyama[e,f], Hiroshi Mori[e,f], Kenji Matsuura[d], Shogo Matsuyama[d,*]

[a] Laboratory of Molecular Cellular Biology, School of Pharmaceutical Sciences, Kobe Gakuin University, 1-1-3 Minatojima, Chuo-ku, Kobe 650-8586, Japan
[b] Laboratory of Toxicology and Safety Science, Graduate School of Pharmaceutical Sciences, Osaka University, 1-6 Yamadaoka, Suita, Osaka 565-0871, Japan
[c] Laboratory of Biopharmaceutical Research, National Institute of Biomedical Innovation, 7-6-8 Saito-Asagi, Ibaraki, Osaka 567-0085, Japan
[d] Faculty of Pharmaceutical Sciences, Himeji Dokkyo University, 7-2-1 Kamiohno, Himeji 670-8524, Japan
[e] Department of Neuroscience, Osaka City University Graduate School of Medicine, Osaka 545-8585, Japan
[f] Core Research for Evolutional Science and Technology, Japan Science and Technology Agency, Japan

## HIGHLIGHTS

- We perform the proteome for $APP_{E693\Delta}$-transgenic mice. Methods are two-dimensional fluorescence difference in gel electrophoresis and mass spectrometry techniques. The expression of 14 proteins are changed in the brain. Aβ oligomers contribute to the expression of proteins.

## ARTICLE INFO

*Article history:*
Received 4 August 2012
Received in revised form 13 October 2012
Accepted 6 November 2012

*Keywords:*
Proteome
Amyloid β oligomers
Alzheimer's disease
Hippocampus
2D-DIGE

## ABSTRACT

We previously identified the E693Δ mutation in amyloid precursor protein (APP) in patients with Alzheimer's disease (AD) and then generated APP-transgenic mice expressing this mutation. As these mice possessed abundant Aβ oligomers from 8 months of age but no amyloid plaques even at 24 months of age, they are a good model to study pathological effects of amyloid β (Aβ) oligomers. The two-dimensional fluorescence difference in gel electrophoresis (2D-DIGE) technology, using a mixed-sample internal standard, is now recognized as an accurate method to determine and quantify proteins. In this study, we examined the proteins for which levels were altered in the hippocampus of 12-month-old $APP_{E693\Delta}$-transgenic mice using 2D-DIGE and liquid chromatography–tandem mass spectrometry (LC–MS/MS). Fourteen proteins were significantly changed in the hippocampus of $APP_{E693\Delta}$-transgenic mice. Actin cytoplasmic 1 (β-actin), heat shock cognate 71 kDa, γ-enolase, ATP synthase subunit β, tubulin β-2A chain, clathrin light chain B (clathrin) and dynamin-1 were increased. Heat shock-related 70 kDa protein 2, neurofilament light polypeptide (NFL), stress-induced-phosphoprotein 2, 60 kDa heat shock protein (HSP60), α-internexin, protein kinase C and casein kinase substrate in neurons protein 1 (Pacsin 1), α-enolase and β-actin were decreased. Western blotting also validated the changed levels of HSP60, NFL, clathrin and Pacsin 1 in $APP_{E693\Delta}$-transgenic mice. The identified proteins could be classified as cytoskeleton, chaperons, neurotransmission, energy supply and signal transduction. Thus, proteomics by 2D-DIGE and LC–MS/MS has provided knowledge of the levels of proteins in the early stages of AD brain.



## 1. Introduction

AD is neuropathologically characterized by abnormal accumulation of extracellular amyloid plaques and intracellular neurofibrillary tangles throughout cortical and limbic regions. Although the current amyloid cascade hypothesis [6] and tau hypothesis [15] provide frameworks for studying AD pathogenesis. Recently, diverse lines of evidence suggest that Aβ peptides play more important roles in AD pathogenesis [13,16,20]. Especially, soluble oligomers of Aβ could be a cause of synaptic and cognitive dysfunction in the early stages of AD. To address the relationship between Aβ oligomers and pathological features of AD, we generated APP transgenic mice expressing the E693Δ mutation, which enhanced Aβ oligomerization without fibrillization [25]. It might provide a clue for elucidating AD pathology caused by Aβ oligomers to analyze the $APP_{E693\Delta}$-transgenic mice.

* Corresponding author. Tel.: +81 79 223 6849; fax: +81 79 223 6857.
*E-mail address:* shogo@himeji-du.ac.jp (S. Matsuyama).

0304-3940/$ – see front matter © 2012 Elsevier Ireland Ltd. All rights reserved.
http://dx.doi.org/10.1016/j.neulet.2012.11.010

One of the most utilized approaches in proteomics to quantify and identify proteins is two dimensional gel electrophoresis (2DE) and mass spectrometry (MS) [5]. Proteomic approaches were most widely based on methods using differential expression on 2D-PAGE gels, or more recently 2D chromatography, followed by mass spectrometry protein identification. Compared to these conventional analyses, 2D-DIGE has higher reproducibility and sensitivity because of its internal standard design which minimizes gel-to-gel variation, improves spot matching, reduces number of gels needed, and permits quantitative analysis of small sample amounts.

In this study, we studied the altered expression of proteins in the hippocampus of $APP_{E693\Delta}$-transgenic mice using 2D-DIGE and LC–MS/MS approach. This approach revealed that the levels of at least 14 proteins were altered in the hippocampus of 12-month-old $APP_{E693\Delta}$-transgenic mice. These findings suggest that Aβ oligomers might cause synaptic and cognitive dysfunction by affecting the expression of these proteins in the hippocampus.

## 2. Experimental procedures

### 2.1. Materials

Sodium dodecyl sulfate, urea, thiourea, CHAPS, dithiothreitol, iodoacetamide, bromophenol blue, and RNase A and DNase I for SDS-PAGE or 2DE were all obtained from Wako Pure Chemical Industries (Osaka, Japan). Source information for all other assay reagents and materials are incorporated into their respective assay methods described below.

### 2.2. Animal subjects

Transgenic mice expressing human $APP_{695}$ with the APP E693Δ mutation under the mouse prion promoter were used [25]. Heterozygous human $APP_{E693\Delta}$-transgenic mice and age-matched non-transgenic littermates were sacrificed at 12 months of age, and their hippocampi were isolated on an ice-cold plate. Animal care and handling were performed strictly in accordance with the Guidelines for Animal Experimentation at Kobe Gakuin University and Himeji Dokkyo University. Every effort was made to minimize the number of animals used and their suffering.

### 2.3. Protein labeling with CyDyes

Equal amounts of total protein from 4 hippocampi of $APP_{E693\Delta}$-transgenic mice or age-matched non-transgenic littermates were separately pooled. Protein samples were labeled with CyDyes (GE Healthcare, Piscataway, NJ), as per manufacturer's instructions. In brief, 50 μg of total protein from each sample was mixed in a tube and labeled with Cy2 minimal dye, and 50 μg protein taken from the mix was used as an internal standard on each gel for the three subsequent 2DE and image analysis. In parallel, 50 μg protein from each sample was labeled with either Cy3 or Cy5, and the dyes scrambled within each group to avoid possible dye bias. As a result, one replicate was Cy3 labeled proteins and another replicate was Cy5 labeled proteins. Two replicates (Cy3 and Cy5 labeled samples) were mixed, divided and applied each three independent gels. The sample volumes were adjusted to 18 μL with labeling buffer (7M urea, 2 M thiourea, 4% CHAPS, 30 mM Tris), followed by addition of 1 μL dye (working solution) to each individual sample. The samples were left on ice for 30 min in the dark, followed by adding 1 μL of 10 mmol/L lysine to stop the reaction.

### 2.4. 2D electrophoresis and image analysis

One sample from each of the CyDye groups was mixed together and adjusted to final concentrations of 1% DTT, 1% IPG buffer at a total volume of 350 μL with lysis buffer (7 M urea, 2 M thiourea, 4% CHAPS) and was used to 24 cm pH 4–7 IPG strips (non-linear; GE Healthcare, Piscataway, NJ) overnight. First dimension isoelectric focusing (IEF) was carried out with IPGphor II (GE Healthcare, Piscataway, NJ). Second dimension SDS-PAGE was performed by mounting the IPG strips onto 20 × 26 cm 12.5% DIGE gels (GE Healthcare, Piscataway, NJ) using Ettan DALT six Large Electrophoresis System (GE Healthcare, Piscataway, NJ) and running the gels at 16 mA/gel for the initial hour and 25 mA/gel at 25 °C constantly until bromophenol blue reached the bottom of the gel. The lysates were labeled at the ratio of 50 μg proteins: 400 pmol Cy3 or Cy5 protein-labeling dye (GE HealthcareBiosciences) in dimethylformamide according to the manufacturer's protocol.

In summary, three analytical gels were completed in total, running 25 μg of pooled reference sample labeled with Cy2, along with two samples (25 μg each), one labeled with Cy3 and the other labeled with Cy5. Gels selected for picking were stained with Deep purple (GE Healthcare, Piscataway, NJ). Approximately 1100 spots were matched across all three analytical gels. The analytical gel was picked using an automated robotic system, Ettan Spot picker (GE Healthcare, Piscataway, NJ). The pick list was created based on the Deep purple image. 2 mm gel plugs were picked, washed, reduced and alkylated, and then digested with trypsin, and the resulting peptides were extracted. Gel trypsinization was performed as previously described [24].

### 2.5. LC/MS/MS identification

Trypsinized peptides were analyzed by nano LC/MS/MS on a ThermoFisher LTQ Orbitrap XL. In brief, 30 mL of hydrolysate was loaded onto a 5 mm 675 mm ID C12 (Jupiter Proteo, Phenomenex) vented column at a flow-rate of 10 mL/min. Gradient elution was conducted on a 15 cm by 75 mm ID C12 column at 300 nL/min. A 30 min gradient was employed. The mass spectrometer was operated in a data-dependent mode, and the six most abundant ions were selected for MS/MS. Mass spectrometry results were searched using Mascot (www.matrixscience.com). Samples were processed in the Scaffold algorithm using DAT files generated by Mascot. Parameters for LTQ Orbitrap XL data require a minimum of two peptide matches per protein with minimum probabilities of 90% at the protein level.

### 2.6. Western blotting

Approximately 25 μg of protein from mouse hippocampus was applied to a 12.5% acrylamide gel and SDS-polyacrylamide gel electrophoresis was performed at 17.5 mA/gel for 2 h in second dimension. The gels were transferred onto PVDF membranes (Pall Corporation, Pensacola, FL, USA), in a trans-blot electrophoresis transfer cell (Nihon Eido, Tokyo, Japan). Western blotting was performed by using monoclonal antibodies against β-actin (diluted 1:1000, Cell Signaling, USA) and clathrin (diluted 1:250, Abcam, USA), polyclonal antibodies HSP60, NFL, voltage-dependent anion-selective channel protein 1 (VDAC) (diluted 1:1000, Cell Signaling, USA) and Pacsin 1 (diluted 1:500, Millipore, USA). Peroxidase-conjugated antibody (diluted 1:5000, Abcam, USA) was used as secondary antibody. The reaction was detected by chemiluminescence with ECL reagents (Pierce Biotechnology, USA). A semi quantitative analysis based on optical density was performed by ImageJ software (available at http://www.rsbweb.nih.gov/ij).

## 3. Results and discussion

The 2D-DIGE gels of the hippocampi from wild type and $APP_{E693\Delta}$-transgenic mice pools were shown as Fig. 1. Two replicates of each pooled sample were run, labeling one replicate with

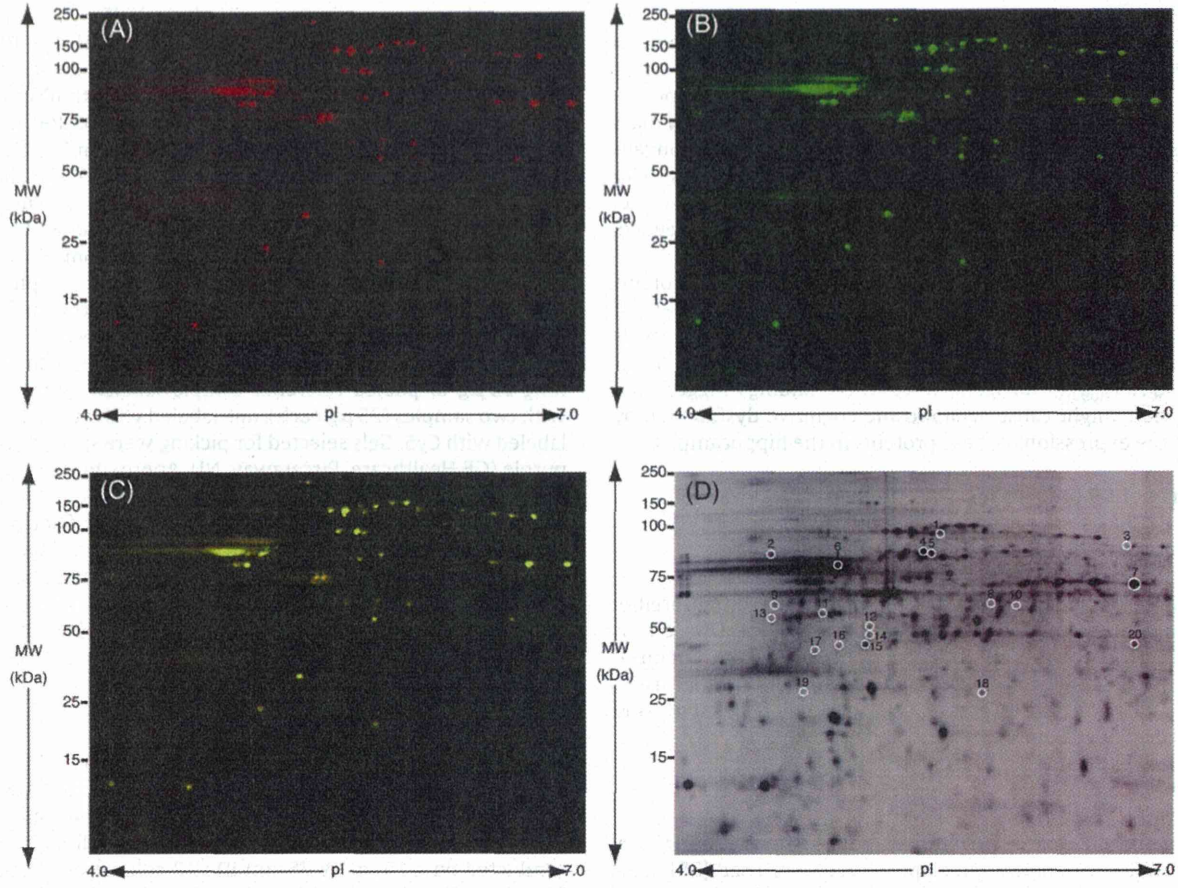


**Fig. 1.** 2D-DIGE gel image of fluorescence-labeled hippocampal proteins of non-transgenic and $APP_{E693\Delta}$-transgenic mice. (A) Analysis of the proteome of non-transgenic mice hippocampi with Cy3 Dye. (B) $APP_{E693\Delta}$-transgenic mice hippocampi with Cy5 Dye. (C) Merged. (D) Fourteen protein spots identified from non-transgenic and $APP_{E693\Delta}$-transgenic mice hippocampi by LC/MS/MS. Black numbers with white circles indicate proteins that are listed in Table 1.

Cy3 (Fig. 1A) and one replicate with Cy5 (Fig. 1B), resulting in three analytical gels. The 2D-DIGE comparative analysis of the wild type and $APP_{E693\Delta}$-transgenic mice revealed significant 74 spots (Fig. 1C). These spots were investigated by LC–MS/MS (Fig. 1D). Finally, fourteen proteins were identified as shown in Table 1. These proteins are classified into several groups that are involved in cytoskeletal, chaperone, energy metabolic, vesicle transport and signaling proteins (Table 2).

Spot nos. 1, 3 and 4 were identified as heat shock-related 70 kDa protein 2, stress-induced-phosphoprotein 1 and HSP60, respectively. The stress-induced-phosphoprotein 1 is the co-chaperone and thought of the function in regulation of interaction with Hsp70 and Hsp90 [10]. HSP60 is the chaperonin which is implicated in mitochondrial protein import and macromolecular assembly and may facilitate the correct folding of imported proteins [9]. The amounts of heat shock-related 70 kDa protein 2, stress-induced-phosphoprotein 1, and HSP60 were significantly decreased. On the contrary, spot no. 9 which was identified as heat shock cognate 71 kDa protein was significantly increased. This protein is also the chaperone and acts as a repressor of transcriptional activation [8]. Thus, Aβ oligomers might contribute to changing the expression of the chaperons.

Spot nos. 8, 10–12 and 16 were identified as actin, and spot nos. 15 and 17 were identified as tubulin β-2A chain. Actin is one of the major cytoskeletal proteins in neurons, and the dynamics of its assembly are involved in many aspects of cell motility, vesicle transport, and membrane turnover [14]. Actin itself is known to link with Aβ, which enhances the neurotoxicity induced by tau-mediated actin filament formation [4]. The four spots of actin but not no. 12 and those of tubulin were significantly increased. Thus, Aβ oligomers might lead to increasing the amounts of actin and tubulin.

Spot nos. 5 and 2 were identified as α-internexin and NFL, respectively, which are known as neuronal intermediate proteins [2,18]. The amounts of α-internexin and NFL were significantly decreased. Thus, the decreased amounts of NFL and internexin might raise neural dysfunction in the hippocampus of AD.

Spot nos. 7 and 13 were identified as α-enolase. Spot nos. 14 and 19 were identified as γ-enolase and ATP synthase subunit β, respectively. Enolase is a multifunctional protein as glycolytic enzyme, belonging to a novel class of surface proteins [11]. ATP synthase is a key role enzyme that provides energy for the cell to use through the synthesis of ATP [1]. The amount of α-enolase was significantly decreased, but the amounts of γ-enolase and ATP synthase subunit β were significantly increased. Interestingly, the levels of α-enolase and ATP synthase subunit α mitochondrial proteins significantly increased in the hippocampus of J20 Tg mice with amyloid deposition [19]. The amyloid deposit enhanced the expression of energy metabolic proteins [22]. Combined with our findings, both Aβ oligomers and amyloid deposition might play an important role in the change of energy metabolic proteins as α-enolase, γ-enolase and ATP synthase subunit β.

Spot no. 20 was identified as dynamin. Dynamin, a well studied neuron-specific mechanochemical GTPase, pinches off synaptic vesicles, freeing them from the membrane and allowing them to re-enter the synaptic vesicle pool to be refilled for future release

**Table 1**
Identified proteins from differentially expressed in the hippocampus of$APP_{E693\Delta}$-transgenic mice when compared to non-transgenic littermates.

| Spot no. | Protein ID | Fold (APP/WT) | *t*-Test | Accession | Coverage | #Peptides | Predicted MW (kDa) | Calc. pI | Score |
|---|---|---|---|---|---|---|---|---|---|
| 1 | Heat shock-related 70 kDa protein 2 | −1.32 | 0.040 | P14659 | 26.22 | 23 | 69.6 | 5.67 | 625.70 |
| 2 | Neurofilament light polypeptide | −1.48 | 0.002 | P08551 | 39.96 | 43 | 61.5 | 4.64 | 1004.84 |
| 3 | Stress-induced-phosphoprotein 1 | −1.44 | 0.002 | Q60864 | 16.21 | 9 | 62.5 | 6.80 | 157.49 |
| 4 | 60 kDa heat shock protein | −1.36 | 0.013 | P63038 | 52.71 | 71 | 60.9 | 6.18 | 1916.39 |
| 5 | Alpha-internexin | −1.34 | 0.023 | P46660 | 42.66 | 39 | 55.7 | 5.27 | 1119.47 |
| 6 | Protein kinase C and cascin kinase substrate in neurons protein 1 | −1.48 | 0.023 | Q61644 | 28.34 | 15 | 50.5 | 5.24 | 356.92 |
| 7 | Alpha-enolase | −1.32 | 0.000 | P17182 | 34.33 | 24 | 47.1 | 6.80 | 474.21 |
| 8 | Actin, cytoplasmic 1 | 1.51 | 0.003 | P60709 | 25.87 | 14 | 41.7 | 5.48 | 231.79 |
| 9 | Heat shock cognate 71 kDa protein | 1.35 | 0.015 | P63017 | 12.54 | 16 | 70.8 | 5.52 | 319.85 |
| 10 | Actin, cytoplasmic | 1.34 | 0.004 | P60709 | 24.27 | 13 | 41.7 | 5.48 | 279.37 |
| 11 | Actin, cytoplasmic 1 | 1.38 | 0.022 | P60709 | 15.47 | 7 | 41.7 | 5.48 | 243.14 |
| 12 | Actin, cytoplasmic 1 | −1.56 | 0.013 | P60709 | 22.67 | 12 | 41.7 | 5.48 | 131.57 |
| 13 | Gamma-enolase | 1.33 | 0.005 | P17183 | 20.05 | 13 | 47.3 | 5.11 | 237.25 |
| 14 | ATP synthase subunit beta | 1.40 | 0.047 | P56480 | 23.60 | 18 | 56.3 | 5.34 | 356.19 |
| 15 | Tubulin beta-2A chain | 1.31 | 0.021 | Q13885 | 14.83 | 13 | 49.9 | 4.89 | 313.07 |
| 16 | Actin, cytoplasmic 1 | 1.47 | 0.002 | P60709 | 6.93 | 3 | 41.7 | 5.48 | 97.01 |
| 17 | Tubulin beta-2S chain | 1.44 | 0.009 | Q13885 | 11.46 | 5 | 49.9 | 4.89 | 118.50 |
| 18 | Clathrin light chain B | 1.68 | 0.005 | P09497 | 8.30 | 3 | 25.2 | 4.64 | 95.06 |
| 19 | ATP synthase subunit beta | 1.46 | 0.013 | P06576 | 16.64 | 16 | 56.5 | 5.40 | 283.06 |
| 20 | Dynamin-1 | 1.40 | 0.006 | Q05193 | 9.61 | 13 | 97.3 | 7.17 | 242.16 |

Mass spectrometry protein identification of 2D-DIGE spots of interest and statistical analysis using *t*-test between wild type mice and $APP_{E693\Delta}$-transgenic mice gels ($P < 0.05$). The proteins of mouse hippocampus were separated by 2DE and identified by LC MS/MS, following in-gel digestion with trypsin. The spots representing identified proteins are indicated in Fig. 1D and are designated with their ID accession numbers of Swiss Prot database. Score relates to the probability assignment. Score and sequence coverage were calculated by MASCOT search engine (http://www.matrixscience.com).

**Table 2**
Functions regulated by proteins that showed an altered expression in $APPE_{693\Delta}$-transgenic mouse hippocampus.

| Function | Identified protein | Up/down |
|---|---|---|
| Cytoskeletal and their interacting proteins | Neurofilament light polypeptide | Down |
| | Alpha-internexin | Down |
| | Actin, cytoplasmic 1 | Up/down |
| | Tubulin β-2A Chain | Up |
| Chaperone and their interacting proteins | Stress-induced-phosphoprotein 1 | Down |
| | 60 kDa heat shock protein | Down |
| | Heat shock cognate 71 kDa protein | Down |
| Energy metabolic proteins | Alpha-enolase | Down |
| | Gamma-enolase | Up |
| | ATP synthase subunit beta | Up |
| Vesicle transport and recycling | Dynamin-1 | Up |
| | Clathrin light chain B | Up |
| Signaling proteins | Protein kinase C and casein kinase substrate in neurons protein 1 | Down |

The analysis of proteins function was done by using MOTIF (http://www.genome.jp/tools/motif/).

[12]. The amount of dynamin was significantly increased. Our findings in $APP_{E693\Delta}$-transgenic mice without plaque deposition are consistent with previous findings that protein levels of dynamin were increased in Tg2576 mice with plaque deposition [21], suggesting that the release of neurotransmitter is affected by dynamin increased irrespective of AD stage. Also, spot no. 6 was identified as Pacsin 1. The Pacsin 1 is colocalized, oligomerized and bound with dynamin, and both proteins participate in synaptic vesicle endocytosis [17]. The amount of Pacsin 1 was significantly increased. Taken together, Pacsin 1 and dynamin enhanced by Aβ oligomers

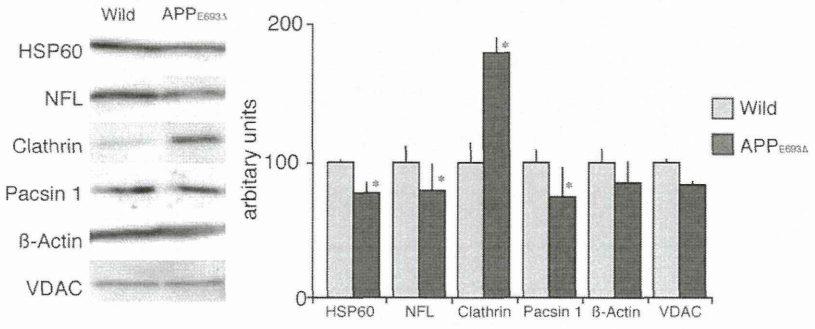


**Fig. 2.** Differentially expressed proteins validated by Western blotting for the hippocampus of non-transgenic and $APP_{E693\Delta}$-transgenic mice. (A) The levels of HSP60, NFL, clathrin, Pacsin 1, β-actin and VDAC in individual samples of each group were detected. (B) Graphical representation of the semi quantitative analysis (mean ± SEM of O.D. of bands). Data are presented as mean ± SEM ($n = 4$) *t*-test; $^*P < 0.05$ vs. $APP_{E693\Delta}$-transgenic mice.

might change the function of synaptic vesicle in the hippocampus of AD.

Spot no. 18 was identified as clathrin, which is known as the major protein of the polyhedral coat of coated pits and vesicles [7]. The amount of spot no. 18 was significantly decreased. APP was associated clusters of clathrin-coated vesicles and endosomes [3]. Thus, Aβ oligomers might inhibit the vesicle formation by clathrin.

In addition, we performed a validation experiment for HSP60, NFL, clathrin, Pacsin 1 and β-actin as the altered proteins, and VDAC as the unchanged protein (as control) [23]. The increased levels of clathrin, the decreased levels of HSP60, NFL, and Pacsin 1 and the unchanged level of β-actin and VDAC in $APP_{E693\Delta}$-transgenic mice hippocampus were validated by Western blotting (Fig. 2).

In summary, we identified the altered levels of 14 proteins in $APP_{E693\Delta}$-transgenic mice hippocampus using 2D-DIGE and LC–MS/MS approach. This approach elucidated the pathological effects of Aβ oligomers on hippocampus. Our findings might provide a clue for investigation of the hippocampus of AD early stage.

## Acknowledgements

This work was supported by grants from Kobe Gakuin University for Collaborative Research C and the Smoking Research Foundation. The authors thank Dr. Tadanori Mayumi for his encouragement during the early days of the study.

## References

[1] U. Andersson, H. Antonicka, J. Houstek, B. Cannon, A novel principle for conferring selectivity to poly(A)-binding proteins: interdependence of two ATP synthase beta-subunit mRNA-binding proteins, Biochemical Journal 346 (Pt 1) (2000) 33–39.
[2] C.L. Chien, R.K. Liem, Characterization of the mouse gene encoding the neuronal intermediate filament protein alpha-internexin, Gene 149 (1994) 289–292.
[3] A. Ferreira, A. Caceres, K.S. Kosik, Intraneuronal compartments of the amyloid precursor protein, Journal of Neuroscience 13 (1993) 3112–3123.
[4] T.A. Fulga, I. Elson-Schwab, V. Khurana, M.L. Steinhilb, T.L. Spires, B.T. Hyman, M.B. Feany, Abnormal bundling and accumulation of F-actin mediates tau-induced neuronal degeneration in vivo, Nature Cell Biology 9 (2007) 139–148.
[5] A. Gorg, C. Obermaier, G. Boguth, A. Harder, B. Scheibe, R. Wildgruber, W. Weiss, The current state of two-dimensional electrophoresis with immobilized pH gradients, Electrophoresis 21 (2000) 1037–1053.
[6] J. Hardy, D.J. Selkoe, The amyloid hypothesis of Alzheimer's disease: progress and problems on the road to therapeutics, Science 297 (2002) 353–356.
[7] J. Hirst, M.S. Robinson, Clathrin and adaptors, Biochimica et Biophysica Acta 1404 (1998) 173–193.
[8] C.R. Hunt, A.J. Parsian, P.C. Goswami, C.A. Kozak, Characterization and expression of the mouse Hsc70 gene, Biochimica et Biophysica Acta 1444 (1999) 315–325.
[9] S. Ikawa, R.A. Weinberg, An interaction between p21ras and heat shock protein hsp60, a chaperonin, Proceedings of the National Academy of Sciences 89 (1992) 2012–2016.
[10] J.L. Johnson, A. Halas, G. Flom, Nucleotide-dependent interaction of Saccharomyces cerevisiae Hsp90 with the cochaperone proteins Sti1, Cpr6, and Sba1, Molecular and Cellular Biology 27 (2007) 768–776.
[11] M. Kaghad, X. Dumont, P. Chalon, J.M. Lelias, N. Lamande, M. Lucas, M. Lazar, D. Caput, Nucleotide sequences of cDNAs alpha and gamma enolase mRNAs from mouse brain, Nucleic Acids Research 18 (1990) 3638.
[12] B.L. Kelly, R. Vassar, A. Ferreira, Beta-amyloid-induced dynamin 1 depletion in hippocampal neurons. A potential mechanism for early cognitive decline in Alzheimer disease, Journal of Biological Chemistry 280 (2005) 31746–31753.
[13] W.L. Klein, G.A. Krafft, C.E. Finch, Targeting small Abeta oligomers: the solution to an Alzheimer's disease conundrum? Trends in Neurosciences 24 (2001) 219–224.
[14] T.B. Kuhn, P.J. Meberg, M.D. Brown, B.W. Bernstein, L.S. Minamide, J.R. Jensen, K. Okada, E.A. Soda, J.R. Bamburg, Regulating actin dynamics in neuronal growth cones by ADF/cofilin and rho family GTPases, Journal of Neurobiology 44 (2000) 126–144.
[15] V.M. Lee, M. Goedert, J.Q. Trojanowski, Neurodegenerative tauopathies, Annual Review of Neuroscience 24 (2001) 1121–1159.
[16] S. Li, S. Hong, N.E. Shepardson, D.M. Walsh, G.M. Shankar, D. Selkoe, Soluble oligomers of amyloid Beta protein facilitate hippocampal long-term depression by disrupting neuronal glutamate uptake, Neuron 62 (2009) 788–801.
[17] J. Modregger, B. Ritter, B. Witter, M. Paulsson, M. Plomann, All three PACSIN isoforms bind to endocytic proteins and inhibit endocytosis, Journal of Cell Science 113 (Pt 24) (2000) 4511–4521.
[18] R.A. Nixon, R.K. Sihag, Neurofilament phosphorylation: a new look at regulation and function, Trends in Neurosciences 14 (1991) 501–506.
[19] R.A. Robinson, M.B. Lange, R. Sultana, V. Galvan, J. Fombonne, O. Gorostiza, J. Zhang, G. Warrier, J. Cai, W.M. Pierce, D.E. Bredesen, D.A. Butterfield, Differential expression and redox proteomics analyses of an Alzheimer disease transgenic mouse model: effects of the amyloid-beta peptide of amyloid precursor protein, Neuroscience 177 (2011) 207–222.
[20] D.J. Selkoe, Alzheimer's disease is a synaptic failure, Science 298 (2002) 789–791.
[21] S.J. Shin, S.E. Lee, J.H. Boo, M. Kim, Y.D. Yoon, S.I. Kim, I. Mook-Jung, Profiling proteins related to amyloid deposited brain of Tg2576 mice, Proteomics 4 (2004) 3359–3368.
[22] R. Sultana, D. Boyd-Kimball, J. Cai, W.M. Pierce, J.B. Klein, M. Merchant, D.A. Butterfield, Proteomics analysis of the Alzheimer's disease hippocampal proteome, Journal of Alzheimer's Disease 11 (2007) 153–164.
[23] M. Takano, K. Maekura, M. Otani, K. Sano, T. Nakamura-Hirota, S. Tokuyama, K.S. Min, T. Tomiyama, H. Mori, S. Matsuyama, Proteomic analysis of the brain tissues from a transgenic mouse model of amyloid beta oligomers, Neurochemistry International 61 (2012) 347–355.
[24] M. Takano, M. Otani, A. Sakai, K. Kadoyama, S. Matsuyama, A. Matsumoto, M. Takenokuchi, M. Sumida, T. Taniguchi, Use of a phosphosensor dye in proteomic analysis of human mutant tau transgenic mice, Neuroreport 20 (2009) 1648–1653.
[25] T. Tomiyama, S. Matsuyama, H. Iso, T. Umeda, H. Takuma, K. Ohnishi, K. Ishibashi, R. Teraoka, N. Sakama, T. Yamashita, K. Nishitsuji, K. Ito, H. Shimada, M.P. Lambert, W.L. Klein, H. Mori, A mouse model of amyloid beta oligomers: their contribution to synaptic alteration, abnormal tau phosphorylation, glial activation, and neuronal loss in vivo, Journal of Neuroscience 30 (2010) 4845–4856.

Life Sciences 91 (2012) 1169–1176

Contents lists available at SciVerse ScienceDirect

Life Sciences

journal homepage: www.elsevier.com/locate/lifescie

# Hypercholesterolemia accelerates intraneuronal accumulation of Aβ oligomers resulting in memory impairment in Alzheimer's disease model mice

Tomohiro Umeda [a,b], Takami Tomiyama [a,b,*], Erika Kitajima [a], Toshiki Idomoto [a], Sachiko Nomura [a,b], Mary P. Lambert [c], William L. Klein [c], Hiroshi Mori [a,b,*]

[a] Department of Neuroscience, Osaka City University Graduate School of Medicine, 1-4-3 Asahimachi, Abeno-ku, Osaka 545-8585, Japan
[b] Core Research for Evolutional Science and Technology, Japan Science and Technology Agency, Japan
[c] Department of Neurobiology and Physiology, Northwestern University, 2205 Tech Drive, Evanston, IL 60208, United States

ARTICLE INFO

*Article history:*
Received 19 August 2011
Accepted 21 December 2011

*Keywords:*
Cholesterol
Intraneuronal Aβ
Synapses
Tau proteins
Memory
Alzheimer's disease
Transgenic mouse

ABSTRACT

*Aims:* Hypercholesterolemia is known to be a risk factor for Alzheimer's disease (AD), and diet-induced hypercholesterolemia has been shown to accelerate amyloid pathology in animals. While growing evidence has shown that synaptic and cognitive dysfunction in AD is associated with intraneuronal accumulation of Aβ, the relationships between hypercholesterolemia, memory impairment, and intraneuronal Aβ remains unclear. The present study aims to clarify this association.

*Main methods:* Transgenic mice expressing amyloid precursor protein (APP) harboring the Osaka (E693Δ) mutation ($APP_{OSK}$-Tg mice) were used. These mice exhibit intraneuronal Aβ oligomers and memory impairment from 8 months of age. Five-month-old male $APP_{OSK}$-Tg mice and non-Tg littermates were fed a high-cholesterol diet for 1 month to induce hypercholesterolemia. At 6 months of age, their cognitive function was evaluated by the Morris water maze. Intraneuronal Aβ, synaptic density, and tau phosphorylation were examined by immunohistochemistry.

*Key findings:* Serum and brain cholesterol levels were significantly higher in $APP_{OSK}$-Tg mice and non-Tg littermates that were fed a high-cholesterol diet than in control mice that were fed normal chow, indicating that hypercholesterolemia was successfully induced. Hypercholesterolemic $APP_{OSK}$-Tg mice, but not control $APP_{OSK}$-Tg mice or hypercholesterolemic non-Tg littermates, exhibited impaired spatial reference memory, which was accompanied with intraneuronal accumulation of Aβ oligomers, reduced synaptophysin immunoreactivity, and abnormal tau phosphorylation in the hippocampus. Hypercholesterolemia-accelerated accumulation of intraneuronal Aβ oligomers was also observed in another model mouse, Tg2576.

*Significance:* Our findings suggest that hypercholesterolemia accelerates intraneuronal accumulation of Aβ oligomers and subsequent synapse loss, resulting in memory impairment.



## Introduction

Extracellular soluble Aβ oligomers are believed to cause synaptic and cognitive dysfunction in Alzheimer's disease (AD) (**Klein et al., 2001; Selkoe, 2002**). However, mounting evidence indicates that intraneuronal accumulation of Aβ is an early event in AD (**Gouras et al., 2000; Fernández-Vizarra et al., 2004**) and Down syndrome (**Gyure et al., 2001; Mori et al., 2002**) and likely contributes to synaptic and cognitive dysfunction (**Wirths et al., 2004; LaFerla et al., 2007; Gouras et al., 2010**). For example, morphological alterations of synapses have been shown to occur in association with intraneuronal accumulation of Aβ in brains of AD patients and Tg2576 mice (**Takahashi et al., 2002**). We also observed that synaptophysin was decreased around the neurons bearing intracellular Aβ in the brains from AD patients (**Ishibashi et al., 2006**). Furthermore, in the triple transgenic 3xTg-AD mice, synaptic and cognitive dysfunction was shown to be correlated with the accumulation of intraneuronal Aβ before amyloid plaque formation (**Oddo et al., 2003; Billings et al., 2005**). Such a correlation of synaptic and/or behavioral abnormalities to intraneuronal Aβ accumulation was also demonstrated in other AD model mice (**Knobloch et al., 2007; Wegenast-Braun et al., 2009; Tampellini et al., 2010**). We also showed that $APP_{OSK}$-Tg mice, which express amyloid precursor protein (APP) harboring the Osaka (E693Δ) mutation (**Tomiyama et al., 2008**), exhibited synaptic and cognitive dysfunction and synapse loss at 8 months of age, the time at which the accumulation of intraneuronal Aβ oligomers without forming amyloid plaques began (**Tomiyama et al., 2010**).

Hypercholesterolemia is known to be a risk factor for AD (**Solomon and Kivipelto, 2009; Stefani and Liguri, 2009**). Cholesterol

* Corresponding authors at: Department of Neuroscience, Osaka City University Graduate School of Medicine, 1-4-3 Asahimachi, Abeno-ku, Osaka 545-8585, Japan. Tel.: +81 6 6645 3921; fax: +81 6 6645 3922.
*E-mail addresses:* tomi@med.osaka-cu.ac.jp (T. Tomiyama), mori@med.osaka-cu.ac.jp (H. Mori).

0024-3205/$ – see front matter © 2012 Elsevier Inc. All rights reserved.
doi:10.1016/j.lfs.2011.12.022

loading of cells inhibits α-secretase (Bodovitz and Klein, 1996) and causes increased Aβ generation via the activation of both β- and γ-secretases (Frears et al., 1999; Xiong et al., 2008), whereas cholesterol depletion results in reduced Aβ production (Simons et al., 1998; Frears et al., 1999; Grimm et al., 2008). In transgenic mice, diet-induced hypercholesterolemia increased Aβ levels in the brain and thus accelerated extracellular amyloid deposition (Refolo et al., 2000; Shie et al., 2002), whereas treatment with statin attenuated amyloid pathology (Petanceska et al., 2002; Kurata et al., 2011). Despite clear evidence of hypercholesterolemia-induced amyloid pathology, the relationship between hypercholesterolemia and memory impairment in animals is somewhat controversial (Fitz et al., 2010; Ullrich et al., 2010; Schreurs, 2010). Furthermore, little is known about intraneuronal Aβ in hypercholesterolemia.

Therefore, in the present study, we investigated the effects of hypercholesterolemia on the level of intraneuronal Aβ and on cognitive function using $APP_{OSK}$-Tg mice. We fed 5-month-old $APP_{OSK}$-Tg mice a high-cholesterol diet for 1 month to induce hypercholesterolemia and examined their phenotypes at 6 months of age when the mice ordinarily show no symptoms or pathology of AD. We found that hypercholesterolemic $APP_{OSK}$-Tg mice displayed earlier onset of cognitive dysfunction, accelerated accumulation of intraneuronal Aβ oligomers, reduced levels of synaptophysin, and abnormal tau phosphorylation in the hippocampus. Our findings suggest that hypercholesterolemia causes memory impairment by accelerating intraneuronal accumulation of Aβ oligomers.

## Materials and methods

### *Antibodies*

Rabbit polyclonal antibody to the N-terminus of Aβ (β001; Lippa et al., 1999) was prepared in our laboratory and was confirmed to bind to both human and mouse Aβ in western blots. Mouse monoclonal antibody NU-1 (Lambert et al., 2007) was used to detect Aβ oligomers. Rabbit polyclonal antibody to the repeat domains of tau (pool 2; Endoh et al., 1993) was prepared in our laboratory and was confirmed to bind to both human and mouse tau in western blots. Mouse monoclonal antibody to phosphorylation at Ser396/Ser404 of tau (PHF-1; Greenberg et al., 1992) was kindly gifted by Dr Peter Davies (Department of Pathology, Albert Einstein College of Medicine, Bronx, NY). Mouse monoclonal antibody to synaptophysin (SVP-38; Sigma, St. Louis, MO) was purchased.

### *Animals*

Five-month-old male $APP_{OSK}$-Tg mice (n = 16) and non-Tg littermates (n = 16) were divided into 2 groups (n = 8 each), such that the mean body weight was not significantly different between the 2 groups. One group was fed a high-cholesterol diet (2% cholesterol and 4% fat; CLEA Japan, Inc., Tokyo, Japan) for 1 month to induce hypercholesterolemia, while the control group was fed normal chow (0.1% cholesterol and 4% fat; CLEA Japan). At the end of the month, blood samples were collected from their tail veins and serum cholesterol levels were measured using the Cholesterol Assay Kit (BioVison, Inc., Mountain View, CA). Three mice of high-cholesterol-fed $APP_{OSK}$-Tg group died during the diet period; hence, this group contained only 5 mice. After behavioral tests, the mice were killed, and their brains were removed for the measurement of brain cholesterol and Aβ and for immunohistochemical analyses of intraneuronal Aβ and synaptophysin. Hippocampal tissues were dissected for measurement of cholesterol levels using the Cholesterol Assay Kit, as described previously (Umeda et al., 2010). In another experiment, 7-month-old male and female Tg2576 mice (n = 6; Taconic, Hudson, NY) were divided into 2 groups (n = 3 each) and were fed high cholesterol diet or normal chow for 1 month. After euthanasia, their brains were removed for immunohistochemical analysis of intraneuronal Aβ. All animal experiments were approved by the committee of Osaka City University and were performed in accordance with the Guide for Animal Experimentation, Osaka City University. Every effort was made to minimize the number of animals used and their suffering.

### *Behavioral tests*

Spatial reference memory was assessed at 6 months of age using the Morris water maze, as described previously (Tomiyama et al., 2010). Male mice were trained to swim to the platform in a pool with a diameter of 96 cm for 5 consecutive days. Training consisted of 5 trials per day with intertrial intervals of 30 s. At day 6, retention of spatial memory was assessed by a probe trial consisting of a 30 s free swim in the pool without the platform. Locomotor activities of the mice were examined by an open-field test, as described previously (Tomiyama et al., 2010). During the period of behavioral tests, mice were maintained on their specified high cholesterol diet or normal chow.

### *Immunohistochemistry*

Mouse brains were fixed in 4% paraformaldehyde, embedded in paraffin, sectioned at 5 μm, and deparaffinized with xylene and ethanol. For Aβ staining only, sections were pretreated by boiling in 0.01 N HCl (pH 2) for 10 min to expose epitopes. After washing with 100 mM Tris–HCl, pH 7.6, 150 mM NaCl (TBS), the sections to be stained with horseradish peroxidase (HRP) were treated with 0.3% $H_2O_2$ for 30 min to inactivate endogenous peroxidases. The sections were then blocked with 20% calf serum in TBS for 1 h. Aβ and tau were stained with corresponding antibodies (β001, NU-1, or PHF-1) followed by biotin-labeled secondary antibodies (Vector Laboratories, Inc., Burlingame, CA), HRP-labeled avidin–biotin complex (Vector Laboratories), and the substrate DAB (Dojindo, Kumamoto, Japan). Synaptophysin was stained with SVP-38 antibody followed by FITC-labeled secondary antibody (Jackson ImmunoResearch Labs Inc., West Grove, PA). The specimens were observed under a BZ-8000 fluorescence microscope (Keyence, Osaka, Japan). Synaptic density in the hippocampal CA3 region was estimated by quantifying synaptophysin fluorescence intensity in an area of 30 μm × 60 μm using NIH imageJ software obtained from a public website (National Institutes of Health; http://rsb.info.nih.gov/nih-image/).

### *Aβ ELISA and tau western blot*

Hemispheres of the cerebral cortex including hippocampus were homogenized by sonication in 4 volumes of TBS containing protease inhibitor cocktail (P8340; Sigma) and phosphatase inhibitor cocktail (06863-01; Nacalai tesque, Kyoto, Japan). 400 μl of the homogenates was centrifuged at 100,000 × *g* at 4 °C for 1 h, and the supernatants were harvested as TBS soluble fractions. The precipitates were dissolved by sonication in 200 μl of 70% formic acid and centrifuged at 100,000 × *g* at room temperature for 1 h. The supernatants were harvested as TBS insoluble fractions and diluted 20-fold in 1 M Tris solution. Aβ concentrations in the TBS soluble and insoluble fractions were determined using human β amyloid (1–40) and (1–42) ELISA kits (298–64601 and 296–64401; Wako Pure Chemical Industries, Ltd., Osaka, Japan). Since $APP_{OSK}$-Tg mice express the mutant Aβ, synthetic Aβ E22Δ peptides were used as standards. The levels of tau were examined by western blot. Aliquots of each fraction were mixed with an equal volume of SDS sample buffer containing β-mercaptoethanol and boiled for 5 min. The samples were subjected to SDS-PAGE (1 μl/lane for TBS soluble fractions and 10 μl/lane for insoluble fractions) with 7% NuPage Tris-Acetate gels (Invitrogen, Carlsbad, CA) and transferred to Immobilon-P membranes (Millipore, Billerica, MA). Total and phosphorylated taus were probed with pool 2 and PHF-1 antibodies, respectively, followed by HRP-labeled second antibodies and the chemiluminescent substrate Immobilon Western (Millipore). Signals were visualized using a LAS-3000 luminescent image analyzer (Fujifilm, Tokyo, Japan).